# Diffusion of iron in copper studied by Mössbauer spectroscopy on single crystals

K. H. Steinmetz and G. Vogl
*Hahn-Meitner-Institut für Kernforschung Berlin, G.m.b.H., Glienicker Strasse 100, Postfach 39 01 28, D-1000 Berlin 39, Federal Republic of Germany and Freie Universität Berlin, D-1000 Berlin 33, Federal Republic of Germany*

W. Petry
*Institut Laue-Langevin, Boîte Postale No. 156X, F-38042 Grenoble Cédex, France*

K. Schroeder
*Institut für Festkörperforschung der Kernforschungsanlage Jülich, G.m.b.H., Postfach 1913, D-5170 Jülich, Federal Republic of Germany*

(Received 30 January 1986)

The broadening of the $^{57}$Fe Mössbauer line due to diffusion jumps of iron atoms in a copper single crystal has been measured as a function of crystal orientation and temperature between 1060 and 1313 K. The results are the following: (i) The anisotropy of the broadening agrees with what is expected for ⟨110⟩ jumps into nearest-neighbor vacancies. (ii) The deviation of the measured anisotropy from the curve predicted for self-diffusion permits the determination of the vacancy jump frequencies in the neighborhood of the iron impurity. The best fit indicates that association and dissociation jumps of the vacancy with or from the impurity are slower, but internal jumps in the vacancy-impurity complex are faster than vacancy jumps in the unperturbed copper lattice. (iii) From the temperature dependence of the resonant intensity (the area of the Mössbauer line) it can be concluded that there is no significant impurity-vacancy binding. (iv) The diffusion coefficient for iron in copper and its temperature dependence are in good agreement with tracer results. At 1313 K, $D=(4.2\pm0.3)\times10^{-13}$ m$^2$/s.

## I. INTRODUCTION

Conventional diffusion investigations are based on measurements of the concentration gradient of diffusing atoms. They determine the average rms distance moved by the atoms in times from minutes to days, using, e.g., radioactive atoms as tracers. We call these "macroscopic" investigations. With Mössbauer spectroscopy, on the contrary, the broadening of the Mössbauer resonance absorption line due to motions of the $\gamma$-emitting or $\gamma$-absorbing atom on the time scale of the nuclear mean lifetime is measured. From the angular dependence of the broadening measured at single crystalline samples, full information on the elementary diffusion jump can be attained. We may therefore call these investigations "microscopic."

The theory for the diffusional broadening of the Mössbauer resonance absorption line has first been worked out by Singwi and Sjölander.[1] These authors have shown that the influence of diffusion on both the emission or absorption probability is essentially given by

$$S(\mathbf{k},\hbar\omega)=\exp(-2W)\frac{1}{\pi}\frac{\Delta\Gamma(\vartheta)/2}{[\Delta\Gamma(\vartheta)/2]^2+(\hbar\omega)^2}, \quad (1)$$

which is of Lorentzian form. $\mathbf{k}$ is the wave vector of the $\gamma$ radiation, $\hbar\omega$ the energy transfer between $\gamma$ radiation and lattice, and $\exp(-2W)$ is the Debye-Waller factor. $\Delta\Gamma(\vartheta)$ is the full width at half maximum (FWHM) of the line broadening due to diffusion jumps as a function of the observation direction:

$$\Delta\Gamma(\vartheta)=\frac{2\hbar}{\tau}A(\vartheta), \quad (2)$$

where $1/\tau$ is the jump frequency and $A(\vartheta)$ is an anisotropic function depending on the scalar products of the $\mathbf{k}$ vector and possible jump vectors. In an experiment the convolution of $S(\mathbf{k},\hbar\omega)$ with the nuclear $\gamma$ line is measured. From the anisotropy $A(\vartheta)$ the elementary jump vectors are deduced by comparison with model calculations.[2]

In this paper the model calculations will be based on the encounter model as worked out for Mössbauer spectroscopy by Wolf *et al.*[3] and generalized to describe diffusion of impurity atoms via vacancies.[4] This model takes advantage of the fact that in metals the vacancy concentration is small. Thus the Mössbauer atom moves through the lattice via successively approaching vacancies each inducing a few jumps of the Mössbauer atom. The line broadening is then formulated in terms of the number of jumps and the final displacements of the Mössbauer atom due to such an encounter.

During the past five years three series of experiments have demonstrated that Mössbauer spectroscopy on single crystals can indeed be used to study the elementary diffusion jump in solids on a microscopic scale.[5–8] The extensive measurements by Petry *et al.*[5] and by Mantl *et al.*[7,8] both have led to new and surprising results. Petry *et al.* studied the dynamics of an iron atom with a

 

trapped interstitial and found a special type of diffusion, namely "localized diffusion" in a cage. Mantl *et al.* studied the normal thermal diffusion of iron in aluminum. From the measured anisotropy of the line broadening they deduced a rather complicated interaction of the iron atom with a vacancy. Unfortunately the results of the conventional tracer-diffusion technique for this system are controversal due to the very low solubility of iron in aluminum, and neither the isotope effect nor the enhancement factor have been measured. This limits the possibilities for comparisons between Mössbauer and tracer results.

Therefore we thought it desirable to study the anisotropy of the diffusional line broadening in a system where diffusion is believed to be well understood on the basis of tracer experiments. We chose a dilute alloy of copper with about 60 at. ppm $^{57}$Co which decays to $^{57}$Fe of which the diffusion was studied.

A first Mössbauer study of the diffusion of $^{57}$Fe in copper single crystals was already performed by Asenov *et al.*[6] These authors measured at one temperature only, i.e., they demonstrated the feasibility of the experiment but did not attempt to draw any detailed conclusions.

The dilute alloy of $^{57}$Co-$^{57}$Fe in copper has several virtues:

(a) We can rely on a series of consistent tracer measurements of iron diffusion in copper[9–11] and can draw conclusions from a comparison with our Mössbauer results.

(b) The isotope effect of iron diffusion in copper[9] and the enhancement of copper diffusion by the addition of solute iron atoms[10] have been measured, and from the results various jump frequencies have been deduced. A comparison with our results can be attempted.

(c) The lattice dynamics of copper has been studied by inelastic neutron scattering up to the melting point,[12] which may help us to explain the temperature dependence of the Debye-Waller factor.

We may therefore expect that Mössbauer measurements of diffusion at the dilute alloy of $^{57}$Co-$^{57}$Fe in copper will permit us to test the extent to which Mössbauer spectroscopy can yield reliable information on the details of impurity diffusion. Furthermore, details of the interaction of Fe impurity and vacancy which are principally undetectable with conventional (macroscopic) methods might be detected by Mössbauer spectroscopy as a microscopic method.

## II. EXPERIMENTAL

Due to intensity reasons Mössbauer measurements of $^{57}$Fe diffusion in a copper single crystal must be carried out as source experiments. That means the specimen itself must be doped with $^{57}$Co. The combination of the high vapor presure of copper close to the melting point and the long measuring time makes it necessary to encapsulate the specimen. To shorten the time of measurement we have used three adsorber-detector systems simultaneously.

### A. Source preparation

A disc of 10-mm diameter and 250-$\mu$m thickness was obtained by spark cutting from a copper single crystal of 99.995% purity with face parallel to the {111} plane. The thickness was reduced by the help of an abrasive technique to about 100 $\mu$m, and finally the disc was chemically etched with a solution of $H_3PO_4$ (70%) to a final thickness of 65 $\mu$m.

The orientation of the specimen was determined by Laue diffraction with an accuracy of $\pm 1°$. By two very fine scratches the orientation was then definitely marked on the specimen. After doping, the specimen was mounted on the sample holder in such a way that the $\langle 001 \rangle$, $\langle 111 \rangle$, and $\langle 1\bar{1}0 \rangle$ directions were parallel to the 180° wide slit of the furnace [see Fig. 1(c)], which defines the measuring plane. By simply moving the detectors in this slit plane measurements could be performed parallel $\langle 001 \rangle$, $\langle 111 \rangle$, and $\langle 1\bar{1}0 \rangle$ directions.

Due to the high activity of the doped specimen the determination of the orientation was done before doping the specimen and fixing it to the holder. Since we could not exclude a small error in the adjustment of the encapsulated specimen to the holder, we checked the orientation after the end of all Mössbauer measurements using a high intensity x-ray diffractometer with good angular resolution ($\leq 0.1°$) keeping the specimen fixed to the sample holder in the same position as for the Mössbauer measurements. The result of this determination of orientation showed that the specimen disc was tilted around its axis ($\langle 111 \rangle$ axis) in such a way, that the plane in which the Mössbauer adsorber-detector systems could be moved formed an angle of 7.8° with the (110) crystal plane, i.e., the plane which includes the $\langle 001 \rangle$, $\langle 111 \rangle$, and $\langle 1\bar{1}0 \rangle$ directions [see Fig. 1(c)]. All model calculations of the anisotropy of the resonance linewidth were done for the so-determined exact sample orientation.

For doping the copper single crystal we used about 50 mCi carrier-free $^{57}CoCl_2$ solved in 0.1$M$ hydrochloric acid solution. This liquid was spread onto the single crystal in drops of 10 $\mu$l each, which were dried by warming up the crystal. When about a quarter of the whole amount of the $CoCl_2$ solution had been deposed on the surface the chlorine was reduced at 593 K in a flowing He-$H_2$ atmosphere for 3 h. $^{57}$Co was then diffused into the crystal at 1225 K for 5 h in the same atmosphere. Subsequently, a further quarter of the $CoCl_2$ solution was spread onto the specimen, etc. Using this step-by-step program we prevented the accumulation of too large a quantity of dried $CoCl_2$ powder on the surface of the specimen.

To receive a homogeneous distribution of cobalt, the source was annealed for 35 h at 1225 K in He-$H_2$ atmosphere. To avoid internal oxidation the heat treatment was terminated in a He-CO atmosphere for 2 h at the same temperature. The specimen was not quenched but cooled down rapidly in a flowing He-$H_2$ gas atmosphere. To check the homogeneity of the cobalt distribution we compared $\gamma$ and induced x-ray emission from both sides of the specimen. The ratio of 14.4 to 6.4 keV lines proved to be identical for both sides. The Mössbauer spectrum at RT showed a single line of Lorentzian shape with a linewidth (FWHM)=0.338 mm/sec versus a Pd—2 at.% $^{57}$Fe absorber. These facts indicate that all cobalt atoms had diffused into the copper lattice and occupied identical sites, which are assumed to be substitutional sites. Etching of the source was not necessary. A comparison of the

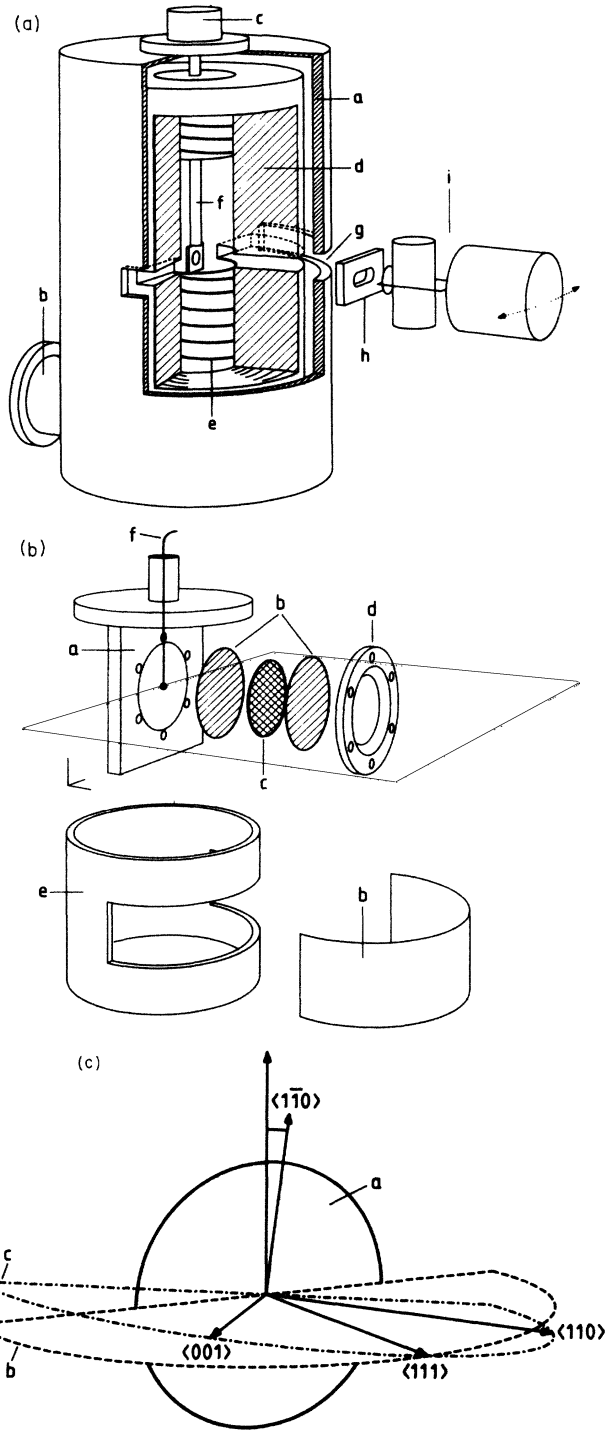


FIG. 1. (a) Simplified drawing of Mössbauer furnace and detector systems. a, watercooled vacuum jacket; b, pumping flange; c, rotary drive; d, insulation, zirconium oxide; e, heating wire on ceramics body, three temperature-controlled zones; f, molybdenum pipe with source holder; g, 180° slit in vacuum chamber and furnace, radiation window: 75-$\mu$m polyamid foil (not shown); h, lead collimator; i, Mössbauer detector and drive system (three systems used simultaneously at different angles, only one is shown). (b) Source holder and encapsulation (simplified). a, molybdenum holder; b, 200-$\mu$m carbon foil; c, source; d, molybdenum ring; e, heat deflector; f, thermocouples. (c) Source orientation as determined by x-ray defraction. a, source; b, detector plane; c, (110) crystal plane.

activity of the source to the activity of the tools which had been used during doping showed that about 80% of the original amount of $^{57}$Co had been brought into the source. That means that the activity of the source was about 40 mCi at the time the Mössbauer diffusion measurements were started. This corresponds to a $^{57}$Co concentration of 60 at. ppm.

### B. Encapsulation of the specimen and temperature control

Long-time measurements at temperatures 45 K below the melting point need special precautions to avoid evaporation. In high vacuum the 65-$\mu$m thick specimen (=source) otherwise would evaporate within less than one day. Even a low rate of evaporation after a while would cause a contamination of the 75-$\mu$m thick polyamid foil used as a radiation window of the sample chamber, and such a contamination (as that of any component visible to the $\gamma$ detectors) would cause additional lines in the Mössbauer spectra. Therefore, we encapsulated the source between two graphite foils of 200-$\mu$m thickness, which were fixed to the molybdenum sample holder like a sandwich [see Fig. 1(b)]. Carbon appears to be an ideal material to encapsulate copper, because there is no solubility of carbon in copper even up to temperatures near the melting point of copper. Besides that, the absorption of the 14.4-keV $\gamma$ rays by 200-$\mu$m carbon is less than 2%. By this gas-tight encapsulation technique the source was protected safely for more than six months at high temperatures and no evaporation was observed. To minimize the temperature gradient the sample holder was surrounded by a molybdenum cylinder whose 180° wide $\gamma$-ray slit was also covered by a 200-$\mu$m graphite foil. The furnace is shown in Fig. 1(a); details of the furnace and the whole setup are described in Ref. 8. To record the temperature of the source, two encapsulated Pt—Pt—10 at. % Rh thermocouples were used, one of which was placed inside the sample holder very close to the rear side of the source. The second one was situated in front of the source close above the measuring plane. After the end of all measurements new thermocouples as well as the thermocouples which had been used during the high-temperature measurements were calibrated at the melting temperature of pure copper. During the measuring time of a high-temperature spectrum ($\sim 4d$) the temperature never changed by more than $\pm 1.5$ K.

### C. Mössbauer spectroscopy

The angular resolution of the Mössbauer spectrometers was determined by lead collimators of $10\times 25$ mm window size in a distance of 170 mm from the source. The resulting resolution function $R(\phi,\vartheta)$ had a trapezoid shape, with areas of $1.1°\times 3.0°$ at the top and $3.7°\times 6.3°$ at the base (smaller values for the direction perpendicular to the plane of the measured anisotropy). All calculated anisotropy curves have been folded with the angular resolution function.

To perform the measurements, three nearly identical transmission spectrometers have been used simultaneously. They were arranged in a common plane defined by the 180° slit of the furnace and could be turned in this plane

around the position of the source within a certain overlapping angular region. By this setup measurements over an angular region of more than 120° are possible.

To get a sufficiently high resonant fraction during the high-temperature measurements (the Debye-Waller factor decreases by about a factor of 7 between RT and 1313 K) absorbers with a rather high $^{57}$Fe concentration (Pd–2 at.% $^{57}$Fe) had to be used, which means that a small broadening of the minimum linewidth had to be accepted. Due to small differences in the $^{57}$Fe concentrations of the absorbers, the measured linewidths at RT of the three detector systems were 0.338, 0.290, and 0.350 mm/sec. The 14.4-keV $\gamma$ rays and the counts of the escape peak of the krypton-gas proportional counters were accumulated. The convention of positive velocity for approaching relative motion between source and absorber is adopted, thus an increase in the electron density at the source nucleus gives rise to a positive change in the central shift.

## III. RESULTS AND DISCUSSION

### A. Mössbauer spectra and their interpretation

In Fig. 2 Mössbauer spectra of $^{57}$Fe in the copper single crystal are shown. Compared to the unbroadened spectrum (973 K) the spectra measured at 1313 K are clearly broadened. The broadening not only depends on the temperature but also on the direction of observation relative to the single-crystal axes. All measured Mössbauer spectra could be perfectly fitted with one Lorentzian only. Different attempts were made to detect an additional superbroad line which could correspond to a resonance of $^{57}$Fe atoms associated to a vacancy during the emission of the $\gamma$ ray ("vacancy line"—compare Ref. 8). But even with high-velocity (up to 50 mm/s) long-time measurements ($3\times10^6$ counts/channel, 1024 channels) we were not able to detect such a superbroad line. This fact may be taken as a first hint that $c_{NN}$ (vacancy concentration in the nearest-neighbor shell of a $^{57}$Fe atom) is not—or at least not much—larger than $c_V$ (vacancy concentration in pure copper).

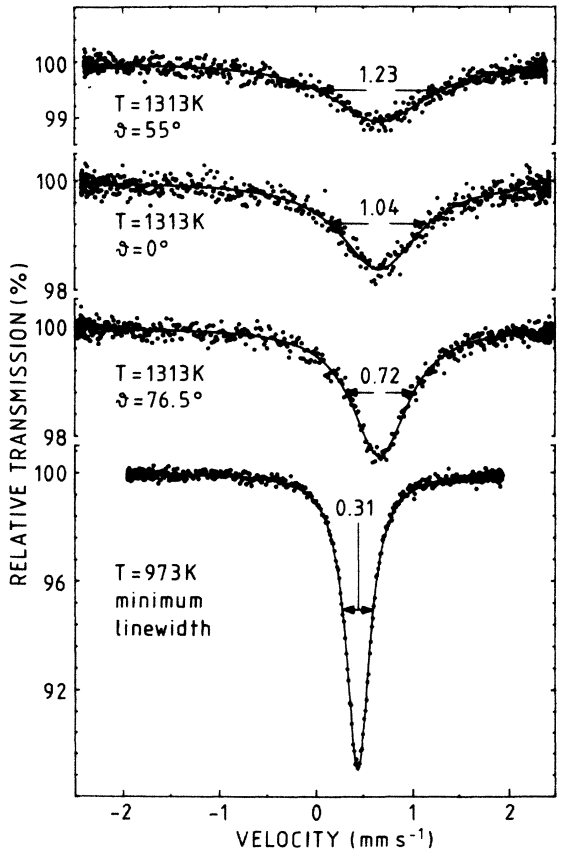


FIG. 2. Mössbauer spectra of $^{57}$Fe in the copper single crystal. Absorber Pd–2 at.% $^{57}$Fe at RT. Notice that the linewidth is different for different directions of observation. $\vartheta$ denotes the measuring angle with respect to the ⟨001⟩ direction.

As a function of temperature, a minimum linewidth was measured between 923 and 973 K. At lower temperatures the Mössbauer lines are slightly broadened. This broadening depends on the pretreatment of the specimen. When the specimen had been cooled down rather fast ($\sim$1 K/s) the linewidth at room temperature (RT) was just about 2% larger than the minimum linewidth, whereas a very slow cooling velocity ($\sim$0.001 K/s) led to a line shape which could not be fitted by a single Lorentzian line. This broadening is caused by the limited solubility of iron in copper. Beside the resonance of $^{57}$Fe in solid solution in copper, at least one further resonance of $^{57}$Fe in an intermetallic copper iron compound appeared when the source had been cooled slowly.

The temperature dependence of the position of the Mössbauer resonance line on the velocity scale (the central shift) is primarily due to the second-order Doppler (SOD) effect which at temperatures above 315 K is described by the Dulong-Petit rule,[13] i.e.,

$$\delta_{\mathrm{SOD}} = -(3E_\gamma k_B T/2mc^2) .$$

Here $\delta_{\mathrm{SOD}}$ is in energy units, $E_\gamma = 14.4$ keV is the Mössbauer $\gamma$ energy and $m$ is the mass of the Mössbauer nucleus. The position of the Mössbauer resonance line as a function of temperature is shown in Fig. 3. The dashed

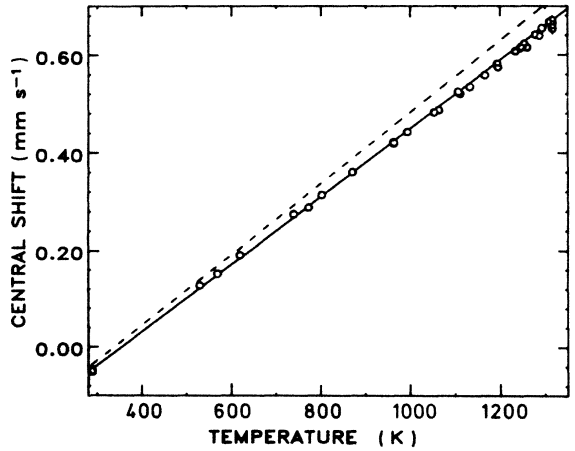


FIG. 3. Central shift of $^{57}$Fe in copper versus temperature. Dashed line: slope ($7.31\times10^{-4}$ mm/s K) given by the Dulong-Petit rule, solid line: measured slope ($7.0\times10^{-4}$ mm/s K).

line represents the slope ($7.31\times10^{-4}$ mm/s K) due to the Dulong-Petit rule. The slope received from a linear fit (straight line) to our data is only $7.0\pm0.1\times10^{-4}$ mm/s K, i.e., at 1313 K the measured central shift is about 0.04 mm/s smaller than expected from the Dulong-Petit rule. This deviation may be partly explained by the increase of the lattice spacing with increasing temperature which reduces the electron density at the position of the nucleus and thus changes the isomer shift.

Such a deviation cannot be explained by softening of the lattice vibrations close to the melting point as may be suggested from the anomalous decrease of the Debye-Waller factor as presented in the next paragraph. The second-order Doppler shift is a measure of the mean-square momentum transfer which becomes completely independent of the dynamical properties of the lattice at $T\gg\Theta_D$.[14]

### B. Temperature dependence of the area of the Mössbauer line

Figure 4 shows the dependence of the resonant fraction $F$ of the 14.4-keV $\gamma$ radiation, i.e., the area of the Mössbauer resonance line, on temperature between room temperature (RT) and 1313 K (i.e., 45 K below the melting point of copper). The fraction is normalized to unity at RT. The actual fraction at RT was about 4–6% depending on which absorber was used.

If no additional Mössbauer resonance line appears, the resonant fraction must follow the temperature dependence of the Debye-Waller factor $e^{-2W}$. For a cubic lattice[15]

$$2W=\frac{\hbar^2}{2m\mathbf{k}^2}\int_0^\infty\frac{1}{\nu}\coth\left[\frac{\hbar\nu}{2k_BT}\right]g(\nu)d\nu, \tag{3}$$

where $m$ is the atomic mass, $\mathbf{k}$ the wave number of Mössbauer $\gamma$ radiation, and $g(\nu)$ the frequency spectrum of lattice vibrations. For temperatures sufficiently larger than the Debye temperature $\Theta_D$ (but practically at all temperatures larger than $\Theta_D$) in harmonic approximation the Debye-Waller exponent, $2W$ is

$$2W=\frac{3\hbar^2\mathbf{k}^2}{k_Bm\Theta_D^2}T\ . \tag{4}$$

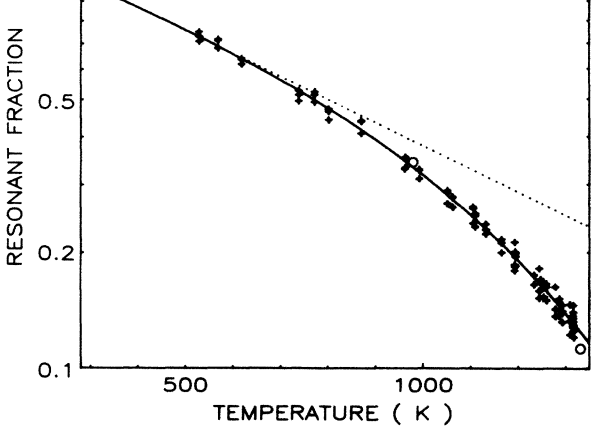


FIG. 4. Temperature dependence of the resonant fraction $F$ of the 14.4-keV $\gamma$ radiation from $^{57}$Fe in the copper single crystal. Solid line: fit to the data $F=\exp(-6E\times T/K_B\Theta_D^2)$ and $\Theta_D=f(T)=338.9-69.7(T/Ts)$ K, $Ts=1358$ K melting temperature of Cu. Straight dotted line: Debye model with $\Theta_D=315$ K. Open circles: values obtained from neutron scattering data on pure Cu (Ref. 12). All values are normalized to the room temperature value.

Figure 4 shows that the actual course of the logarithm of the resonant fraction does not follow a linear dependence on $T$ as should be expected from Eq. (4) (dotted line, with $\Theta_D=315$ K for copper[16]) but rather becomes increasingly steeper with increasing temperature. Since we perform source experiments this strong decrease of the resonant fraction cannot be explained by a leaking encapsulation and eventually evaporation of $^{57}$Co. A possible reason for this deviation from linearity is an anharmonicity of the lattice vibrations. To our knowledge copper is the only substance for which the frequency spectrum of lattice vibrations has been measured by neutron scattering at temperatures up to the region of the melting point.[12] A considerable temperature dependence, i.e., anharmonicity has been found. Following calculations by Schober and Dederichs[15] we have deduced the Debye-Waller factor for the three temperatures for which neutron scattering measurements have been done assuming that iron atoms in copper vibrate in the same way as host atoms. From Fig. 4 it can be seen that the so-calculated values (open circles) fit the experimental data well. This implies that the strong downward curvature of the measured area of the Mössbauer resonance line is compatible with the anharmonicity in the lattice vibrations. We therefore conclude that the fraction of iron atoms bound at any moment to vacancies is immeasurably small. If it were larger we would expect to find a further reduction of the area by a factor

$$1-12c_{\mathrm{NN}}=1-12c_V\exp(E_b/k_BT)$$

due to the appearance of a very broad, and therefore unobservable, vacancy line (compare Ref. 7) where $E_b$ is the binding energy between iron impurity and vacancy. With a vacancy concentration $c_V=1.5\times10^{-4}$ at 1313 K (Ref. 17) we can estimate that $E_b$ is smaller than 0.1 eV.

It may be worthwhile stressing again that this investigation into copper profits from the fact that copper is a well-investigated substance, better studied than probably any other metal. In evaluating the Debye-Waller factor measurements we profit in particular from the results of measurements of the frequency spectrum of lattice vibrations up to the melting point. As mentioned above, such measurements have not been taken for any other substance. The earlier Mössbauer study of the diffusion of iron in aluminum[8] suffered from the unavailability of such data.

### C. Diffusional broadening of the Mössbauer resonance line

Figure 5 shows the experimental data of the diffusional broadening of the Mössbauer resonance line measured at 1313 K as a function of the observation direction relative

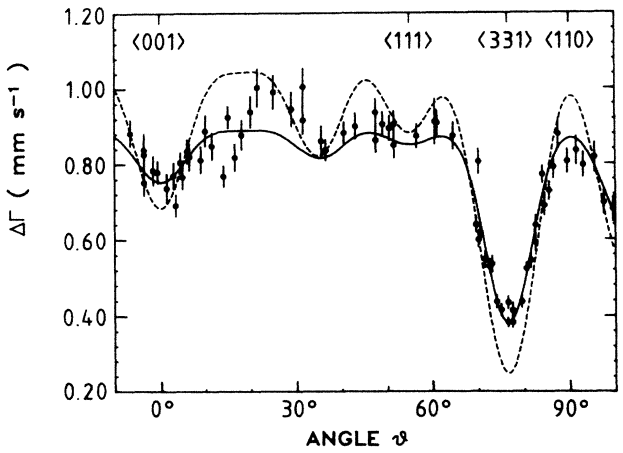


FIG. 5. Diffusional broadening $\Delta\Gamma(\vartheta)$ of the resonance line as a function of the observation direction at $T=1313$ K. $\vartheta$ denotes the angle between the ⟨001⟩ crystal axis and observation direction. Dashed line: computer simulation for self-diffusion in copper (parameters in Table I, No. 1). Solid line: simulation for diffusion of $^{57}$Fe in copper which agrees best with measured data (parameters in Table I, No. 4). All simulations have been convoluted with the experimental resolution.

to the ⟨001⟩ direction of the single crystal. As described in Sec. II A the observation plane, i.e., the plane in which the Mössbauer absorber-detector systems can be moved, is a plane tilted by 7.8° around the ⟨111⟩ direction [see Fig. 1(c)]. Therefore, the symbols for crystal directions in Fig. 5 are not exact (except the ⟨111⟩ direction), but rather indicate an approximate direction. All model calculations were done with the real crystal orientation. Measurements which yielded a central shift or resonant fraction deviating from the average value of all measurements by more than 1.5 times the standard deviation have been eliminated because deviations of this size indicate that some uncontrolled vibrations had disturbed data collection. In spite of installation of the complete device on an air-cushion support, such perturbations could not be completely excluded for this measurement series lasting for nearly one year. From 80 measurements at 1313 K altogether, 9 measurements had to be eliminated.

Monte Carlo simulations of the jumps of the impurity and the vacancy have been performed in order to determine the anisotropy of the broadening of the Mössbauer resonance line for various combinations of jump frequencies. We have used the computer program developed by Schroeder[4] for impurity jumps in fcc hosts which is based on the original program by Wolf and Differt[3] for self-diffusion.

The program simulates encounters of a vacancy and a Mössbauer atom (MA), and calculates the resulting distribution of the displacements of MA's by examining a large number ($>2000$) of encounters. Every simulated encounter starts with a vacancy on a nearest-neighbor (NN) site to the MA. The vacancy then jumps randomly to one of its neighboring sites, the probability of which jump is performed depending on the corresponding jump frequency. In consequence, the MA itself will jump to a NN site with a certain probability. During the following jumps of the vacancy the MA may move again, but if the vacancy leaves the next-nearest-neighbor (NNN) sphere of the MA, the probability of its returning to the MA decreases rapidly. Therefore, the encounter is considered to be finished after 2000 jumps of the vacancy.

The encounter model[3] which is the basis of these simulations looks only at the consequences of an encounter of the Mössbauer atom with a vacancy, i.e., it examines how many and which displacements of a Mössbauer atom occur during an encounter. The model regards the time spent during the encounter as negligibly short compared with the time the Mössbauer atom spends without a vacancy; therefore, the model does not show what happens during the encounter. As a result of the simulation we receive $W_{\mathrm{enc}}(\mathbf{R}_n)$ which is the probability that after the end of the encounter the Mössbauer atom is displaced by a vector $\mathbf{R}_n$. Therefore, $\sum_n W_{\mathrm{enc}}(\mathbf{R}_n)\exp(i\mathbf{k}\mathbf{R}_n)$ is a structure factor describing the matching of the phases of the $\gamma$ wave emitted from the site occupied by the Mössbauer atom at the start of the encounter and from the site occupied at its end. The simulation further yields $z_{\mathrm{enc}}$ which is the average number of jumps of the impurity during the encounter and the correlation factor $f$:

$$f=\frac{1}{z_{\mathrm{enc}}}\sum_n W_{\mathrm{enc}}(\mathbf{R}_n)\frac{|\mathbf{R}_n|}{d}, \tag{5}$$

which describes the probability that a series of jumps does not lead back to the original site ($d$ equals the NN distance). The anisotropy of the diffusional broadening of the Mössbauer resonance line results to[3]

$$A(\vartheta)=\frac{1-\sum_n W_{\mathrm{enc}}(\mathbf{R}_n)\exp(i\mathbf{k}\mathbf{R}_n)}{z_{\mathrm{enc}}}. \tag{6}$$

The physical meaning of Eq. (6) may be understood as follows. In case of exact phase matching between all the wave trains emitted from start and end site,

$$\sum_n W_{\mathrm{enc}}(\mathbf{R}_n)\exp(i\mathbf{k}\mathbf{R}_n)$$

would equal 1 and the Mössbauer resonance line would be unbroadened. In three-dimensional reality, however, there is no crystal direction for which the structure factor becomes 1: the resonance line is rather broadened in all directions, the size of the broadening varying markedly with $\vartheta$.

According to Eq. (2) the diffusional broadening of the Mössbauer resonance line is related to the jump frequency $1/\tau$ and the possible jump vectors $\mathbf{R}_n$ of the Mössbauer atom. This permits us to determine the jump frequency $1/\tau$ by comparing the simulation results with the measured size of the broadening and its anisotropy.

The diffusivity $D$ follows then from the Einstein-Smoluchowski equation

$$D=\frac{d^2}{6\tau}f, \tag{7}$$

where $d$ is the jump distance.

In Refs. 4 and 7 the parameters $W_{\mathrm{enc}}(\mathbf{R}_n)$, $z_{\mathrm{enc}}$, and $f$

TABLE I. Parameters for encounters in fcc crystals. $W_{enc}(R_n)$ is the probability that a tracer, which started on (000) ends on a certain lattice site after the end of an encounter, $\sum_n W_{enc}(R_n)=1$ (take regard of the different number of atoms per shell). No. 1: self-diffusion, No.4: simulation, which fits best to measured data.

| No. | $w_1/w_0$ | $w_2/w_0$ | $w_{int}/w_0$ | $w_{34}/w_0$ | $f$ | $z_{enc}$ | $fz_{enc}$ | $R_n=0=(000)$ | $w_{enc}(R_n)$ $(10^{-1}$ %) (110) | (200) | (211) | (220) | Sum of all $R_n \geq (310)$ |
|---|---|---|---|---|---|---|---|---|---|---|---|---|---|
| 1 | 1 | 1 | 0.5 | 1 | 0.7804 | 1.3314 | 1.039 | 82.21 | 71.24 | 3.43 | 1.35 | 0.56 | 3.17 |
| 2 | 4.5 | 1.39 | 1.06 | 0.02 | 0.7617 | 11.115 | 8.466 | 25.50 | 19.71 | 8.08 | 5.37 | 4.50 | 506.5 |
| 3 | 4.5 | 1.34 | 1.04 | 0.05 | 0.7878 | 5.063 | 3.989 | 43.00 | 32.83 | 11.92 | 6.85 | 4.37 | 274.5 |
| 4 | 4.5 | 1.33 | 1.04 | 0.1 | 0.7918 | 3.211 | 2.542 | 53.00 | 43.04 | 14.00 | 6.31 | 3.54 | 152.5 |
| 5 | 4.5 | 1.33 | 1.04 | 0.2 | 0.7927 | 2.150 | 1.704 | 64.00 | 55.38 | 5.17 | 4.94 | 2.67 | 59.0 |
| 6 | 4.5 | 1.26 | 0.98 | 0.6 | 0.8396 | 1.555 | 1.306 | 60.5 | 64.75 | 6.50 | 3.56 | 1.5 | 20.0 |

had been determined by Monte Carlo simulations of the encounter based on the "five-frequency model" of Lidiard, LeClaire,[18] and others. In that model $w_0$ is the vacancy jump frequency in the host lattice sufficiently far away from an impurity. Furthermore $w_1$ and $w_2$ are the frequencies of vacancy jumps in the impurity's nearest-neighbor shell and of exchange jumps of impurity and vacancy, thus $w_1$ and $w_2$ describe the jumps *within* the impurity-vacancy complex. Finally, $w_3$ and $w_4$ are the frequencies of vacancy dissociation and association jumps *from or to* the nearest neighbor shell of the impurity.

In the present work we base the interpretation of our measurements on a simpler situation. We have deduced in Sec. III B that there is no binding between iron impurity and vacancy, i.e., the nonlinear decay with temperature of the Debye-Waller exponent is fully explained by anharmonic effects. Consequently, the frequencies of association $w_4$ and of dissociation $w_3$ between impurity and vacancy are equal; we call them $w_{34}$.

In addition, we introduce a simplification of the five-frequency model. We define an effective internal frequency $w_{int}$ of the impurity-vacancy encounter

$$w_{int}=\frac{w_1 w_2}{w_1+w_2} . \tag{8}$$

$w_{int}$ describes the jumps in the impurity-vacancy complex. The reason for this simplification of the five-frequency model is the following: Our fitting results show that we can barely distinguish between separate influences of $w_1$ and $w_2$ on the anisotropy and the absolute value of the broadening of the Mössbauer resonance. This will be shown later in the paper.

In Fig. 5 the dashed line presents the line broadening as determined by computer simulation for the case of self-diffusion, i.e., in the case of equality of all five frequencies in the five-frequency model. The curve has been convoluted with the resolution function of our detector system in order to permit direct comparison with the measured data. Obviously, the anisotropy of the data (i.e., the oscillations in the size of the line broadening) is smaller than expected for self-diffusion.

The solid line in Fig. 5 is the result of the simulation (again convoluted with the resolution function) which agrees best with our measured data. It corresponds to $w_{int}=1.0w_0$, $w_{34}=0.1w_0$, $z_{enc}=3.2$, $f=0.79$, and $W_{enc}(R_n)$ as given in Table I. With Eqs. (2), (6), and (7) and $d=0.2609$ nm the diffusivity is as follows:

$$D(1313\text{K})=(4.2\pm0.3)\times10^{-13}\ \text{m}^2/\text{s} .$$

In the following we shall perform a comparison of the measured data with a series of anisotropy curves as calculated by help of Monte Carlo computer simulations in order to demonstrate that the definition of the internal jump frequency $w_{int}$ really makes sense, and to give a feeling for the limits of uncertainty within which the jump frequencies can be determined.

First we have kept $w_{34}$ and $w_{int}$ fixed at their values for the best fit to the data ($w_{34}=0.1w_0$, $w_{int}=1.0w_0$), whereas $w_1$ and $w_2$ (i.e., the constituents of $w_{int}$) have been varied. It turned out that varying the ratio $w_1$:$w_2$

between 0.5 and 10 has no significant influence on the anisotropy. We can get a qualitative understanding of this insensibility: What mainly matters for the strength of the anisotropy are $w_{int}$ and $w_{34}$, i.e., whether we have a "vivid internal life" of the encounter before the vacancy dissociates again. Details of the "internal life" have only minor influence on the absolute value of the anisotropy of the line broadening.

Next we have kept $w_{34}$ fixed at its best value ($w_{34}=0.1w_0$), and $w_{int}$ has been varied between $0.5w_0$ and $2w_0$. From the comparison of the simulations and the data we estimate that the uncertainty in $w_{int}$ is

$$0.9w_0 \leq w_{int} \leq 1.1w_0 \ .$$

Finally, we have kept $w_{int}$ fixed at its best value ($w_{int}=1.0w_0$) and have varied $w_{34}$. For this set of simulations the result are shown in Fig. 6. Comparison shows that $w_{34}$ values in the range $0.08w_0 \leq w_{34} \leq 0.12w_0$ are compatible with the measured data.

Summarizing, we can state that $w_{int}$ is a reasonable definition and $w_{int}$ and $w_{34}$ can be determined from fitting the anisotropy of $\Delta\Gamma$ within the following limits:

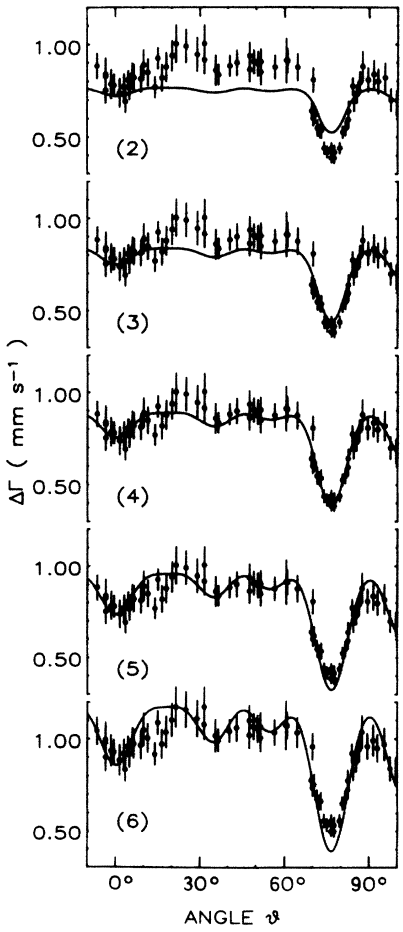


FIG. 6. Examples for simulations with different sets of frequencies as given in Table I, Nos. 2–6. $w_{int}$ is kept fixed to $w_{int}=1.0w_0$. $w_{34}$ from top to bottom is $0.02w_0$, $0.05w_0$, $0.1w_0$, $0.2w_0$, $0.6w_0$. $z_{enc}f(2)=8.5$, $z_{enc}f(3)=4.0$, $z_{enc}f(4)=2.5$, $z_{enc}f(5)=1.7$, $z_{enc}f(6)=1.3$.

$0.9w_0 \leq w_{int} \leq 1.1w_0$ and $0.08w_0 \leq w_{34} \leq 0.12w_0$. Let us summarize the physics which is hidden behind the simulations of the anisotropy function $\Delta\Gamma(\vartheta)$. We try to do so by considering which physical parameters determine the anisotropy and in which way they do act. It is evident that the anisotropy of the diffusional line broadening will be weaker the wider the distribution of impurities (the Mössbauer atoms) at the end of the encounters is. Expressed the other way round, the anisotropy will be most pronounced if every encounter transports the impurity just to a nearest-neighbor site (see Ref. 18). What determines the width of that distribution? It depends on the number of jumps during an encounter which are efficient (not leading back to the original site) $z_{enc}f$. Thus we expect that the anisotropy will be weaker the larger $z_{enc}f$ is. From Fig. 6 and Table I it can be seen that indeed this relation holds: The smearing out of the anisotropy curve is stronger the larger $z_{enc}f$ is.

For small $w_{34}$—as is the case here—the displacement of the Mössbauer atom occurs as a result of a collaboration between $w_1$ and $w_2$ jumps. This "collaboration" of $w_1$ and $w_2$ is necessary to create a vivid internal life in the encounter and, thus, an effective transport of the impurity. An extreme ratio of $w_1$:$w_2$ (either very large or very small) would not be effective because either the vacancy would circle around the impurity without a reaction of the impurity ($w_1 \gg w_2$) or the impurity would frequently just exchange with the vacancy jumping to and fro without a further-leading transport ($w_2 \gg w_1$). We claim that the effectiveness of the internal life in the encounter is well described by the choice of $w_{int}=w_1w_2/(w_1+w_2)$. The length of an encounter is determined by the ratio of $w_{int}$ and $w_3$; in detail, the smaller $w_3$ compared to $w_{int}$, the longer the encounter is, giving the impurity atom the opportunity to jump several times before the vacancy dissociates again.

From tracer studies it is possible to deduce various ratios of jump frequencies making use of measurements of the enhancement factor and the isotope effect. A comparison of these ratios as given by Bocquet[10] with the corresponding ratios deduced from our measurements is given in Table II. $w_3/w_1$ as determined by Bocquet agrees well with $w_3/w_{int}$, whereas we find a lower value than Bocquet for $w_4/w_0$. The ratio $w_2/w_1$ we can only determine within a wide range not in conflict with Bocquet's value.

Recently Ruebenbauer[19] performed computer simulations of the anisotropic line broadening for impurity diffusion on the basis of the encounter model. In principle, his work reproduces the results of Schroeder.[4] For systems with a low vacancy binding energy like Fe in Cu he proposes a simplified approach in a high-temperature limit. Neglecting different entropies for different frequencies, this limit yields $w_3/w_1=w_4/w_0=1$ and $w_2/w_1=(m_{imp}/m_{host})^{1/2}=0.95$ for $Cu^{57}Fe$ ($m_{imp}$,$m_{host}$ equals the mass of the impurity and host, respectively), i.e., the only difference to self-diffusion comes from the different masses. Ruebenbauer's model yields results which are in discrepancy with Bocquet's and our values as well.

Please note finally that the jump distance $d$ corresponding to one elementary jump is, in principle, a free parame-

TABLE II. Comparison of frequency ratios resulting from tracer studies (see Bocquet, Ref. 10) and from this work.

| | $w_3/w_1$ | $w_4/w_0$ | $w_2/w_1$ |
|---|---|---|---|
| Tracer | 0.09±0.03 | 0.30±0.04 | 0.35±0.15 |
| | $w_3/w_{int}$ | $w_4/w_0$ | $w_2/w_1$ |
| This work | 0.10±0.02 | 0.10±0.02 | $0.1 < w_2/w_1 < 2$ |

ter in the simulations of the anisotropy, because the positions of the extreme of the anisotropy curve are related to $d$. From comparison with the simulations we get

$$d = 0.26 \pm 0.01 \text{ nm}$$

in agreement with the nearest-neighbor distance in copper at 1313 K $d = 0.2609$ nm.

### D. Temperature dependence of line broadening and comparison with literature on tracer results

For temperatures different from 1313 K we have measured the line broadening $\Delta\Gamma$ for only eight representative single-crystal directions. Fig. 7(a) gives the results for three of these, showing that the Arrhenius plots are parallel within the accuracy of our measurements. The same holds for the directions not shown. This implies that the anisotropy stays the same between 1060 and 1313 K. It follows that the relation between the jump frequencies stays the same over this temperature range, i.e., the jump mechanism is temperature independent.

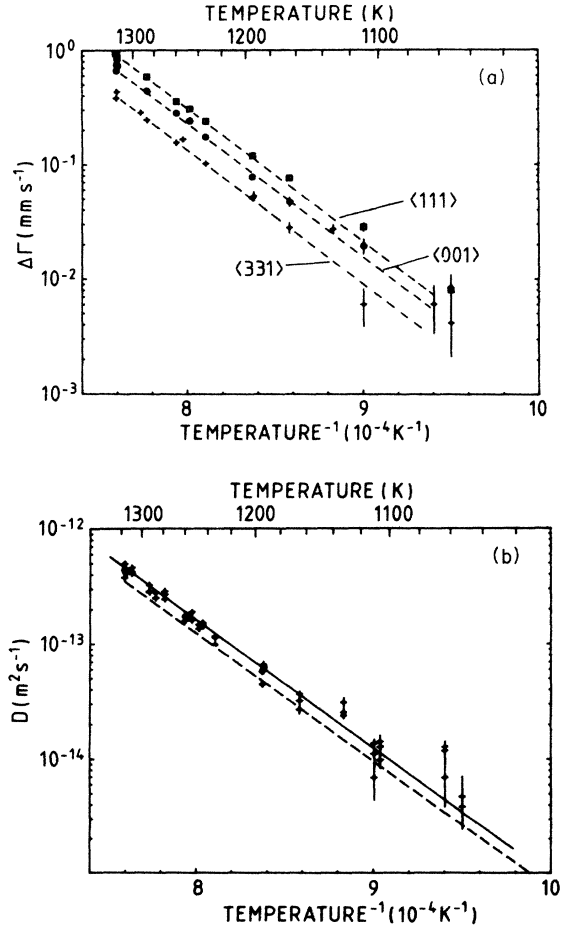


FIG. 7. (a) Temperature dependence of the diffusional line broadening for $^{57}$Fe in a copper single crystal for three different directions of observation. (b) Diffusion coefficient for $^{57}$Fe in copper determined from the anisotropic line broadening. Solid line: fit to the measured data; dashed line: tracer data (Ref. 11).

With the help of Eqs. (2), (6), and (7) the anisotropic $\Delta\Gamma$ measured for the different directions has been converted to an isotropic diffusion coefficient. Figure 7(b) compares the diffusivities so determined with tracer data of various authors.[9–11] The agreement is satisfactory. The activation energy is 2.24±0.02 eV in agreement with the tracer value 2.24±0.01 eV. The prefactor $D_0$ is slightly larger than that deduced from tracer studies: $D_0$(Mössbauer) $= (1.67 \pm 0.2) \times 10^{-4}$ m$^2$/s, $D_0$(tracer) $= (1.2 \pm 0.2) \times 10^{-4}$ m$^2$/s. We do not think that this difference is significant.

## IV. SUMMARY AND CONCLUSIONS

The principal results of this work are as follows:

(i) The anisotropy of the line broadening, i.e., the angles for which maximum and minimum line broadening is found, agrees perfectly with what is expected for ⟨110⟩ jumps into NN vacancies.

(ii) From the deviation of the anisotropy from the curve predicted for self-diffusion, jump frequencies of the Fe-impurity-vacancy complex can be deduced. We have deduced the internal jump frequency $w_{int}$ of the complex at 1313 K as $w_{int} = (1.0 \pm 0.1) w_0$, i.e., the jumps in the complex are about as fast as jumps of the vacancy in the pure copper lattice, the real uncertainty in the value being probably higher. A separate determination of impurity-vacancy exchange jumps and vacancy jumps in the NN shell of an impurity, both together constituting $w_{int}$, does not appear to make sense, since the anisotropy is rather insensitive to a mutual change of $w_1$ and $w_2$ as long as $w_{int}$ stays the same.

(iii) The enhanced temperature dependence of the resonant fraction can be fully accounted for by the softening of the phonon spectrum as determined by neutron scattering in pure copper. The binding effect between a vacancy and an Fe atom can only be small (binding energy of less than 0.1 eV). We have assumed no binding and have set the frequencies for vacancy association to and dissociation from the impurity equality. From the anisotropy we obtain $w_{34} = (0.10 \pm 0.02) w_0$, i.e., association and dissociation jumps are about ten times slower than vacancy jumps in pure copper. This value is only one third of the value deduced from tracer diffusion measurements.

The real error is probably higher than 20%. If we interpret the change of the jump frequencies as changes of barrier heights we arrive at a schematic picture of a potential seen by a vacancy in the neighborhood of an Fe impurity in copper as sketched in Fig. 8.

(iv) The diffusion coefficients determined by Mössbauer spectroscopy and tracer diffusion technique agree in activation energies: $2.24\pm0.02$ eV and $2.24\pm0.01$ eV, respectively. There is a slight, but probably not significant, difference in the $D_0$ values which are $(1.67\pm0.2)\times10^{-4}$ m$^2$/s and $(1.2\pm0.2)\times10^{-4}$ m$^2$/s.

(v) From the temperature dependence of the line broadening in different directions it follows that the frequency ratios $w_i/w_0$ remain unchanged between 1060 and 1313 K.

This study on a system well investigated with the tracer technique has proved that the results of the diffusional Mössbauer line broadening at single crystals are in satisfactory agreement with results from tracer diffusion studies. Different from the tracer technique quasielastic Mössbauer spectroscopy yields direct information on the jump mechanism as jump vectors and jump frequencies. The study has shown the limits within which these frequencies can be determined, e.g., by demonstrating that a separate determination of $w_1$ and $w_2$ is possible only within wide limits if $w_{34}$ is small.

In our opinion the future of studies looking into diffusional line broadening in single crystals does not primarily lie in determining separately the various jump frequencies involved in a diffusion process, the five-frequency model being an oversimplification anyway. We rather believe that Mössbauer studies of this type may contribute to the understanding of unexplained diffusion mechanisms where even the elementary jump vector is unknown. These are, e.g., fast-diffusion processes where an interstitial mechanism is under discussion or diffusion processes in more complicated lattices than fcc and bcc metal lattices. We hope that this study of a simple system has contributed to solidifying the basis for such studies of more complicated (and perhaps more interesting) systems.

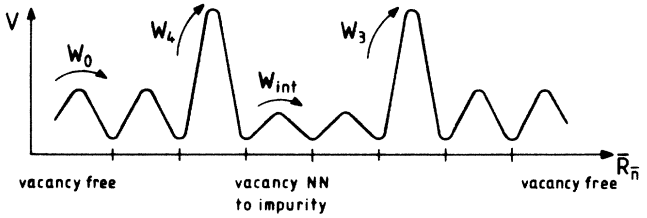


FIG. 8. Schematic representation of the potential seen by a vacancy in the neighborhood of an Fe impurity in copper. The association frequency $w_4$ is much smaller than $w_0$ ($w_4=0.1w_0$), i.e., a vacancy feels a repulsion when approaching an Fe impurity. But once the vacancy has arrived in the nearest-neighbor shell of the Fe impurity the complex can perform quite a number of jumps ($w_{\text{int}}=2w_0=20w_{34}$) before the vacancy leaves again, i.e., impurity and vacancy behave like they are in a "cage" rolling through the lattice for about 20 jumps. There is no vacancy impurity binding, i.e., the association and dissociation frequency are equal, $w_3=w_4=w_{34}$.

## ACKNOWLEDGMENTS

We are grateful to Professor Ch. Herzig, Institut für Metallforschung, Münster, for critical comments and fruitful discussions. We thank Professor E. Nembach, Institut für Metallforschung, Münster, for providing us with the copper crystal and H. Bleif for help with the x-ray determinations of crystal orientation. This work was supported by the Deutsche Forschungsgemeinschaft (Bonn, Germany) via Sonderforschungsbereich 161 (Hyperfeinwechselwirkungen).

[1]K. S. Singwi and A. Sjölander, Phys. Rev. **120**, 1093 (1960).
[2]C. T. Chudley and R. J. Elliot, Proc. Phys. Soc. London **77**, 353 (1961).
[3]D. Wolf, Appl. Phys. Lett. **30**, 617 (1977); D. Wolf and K. Differt, Comput. Phys. Commun. **13**, 167 (1977); D. Wolf, K. Differt, and H. Mehrer, Comput. Phys. Commun. **13**, 183 (1977).
[4]K. Schroeder, D. Wolf, and P. H. Dederichs, in *Point Defects and Defect Interactions,* edited by J. I. Takamura, M. Doyama, and M. Kiritani (University of Tokyo Press, Tokyo, 1982), p. 570, and (unpublished).
[5]W. Petry, G. Vogl, and W. Mansel, Phys. Rev. Lett. **45**, 1862 (1980); Z. Phys. B **46**, 319 (1982).
[6]S. Asenov, T. Ruskov, T. Tomov, and I. Spirov, Phys. Lett. **79A**, 349 (1980).
[7]S. Mantl, W. Petry, and G. Vogl, in *Nuclear Physics Methods in Materials Research,* edited by K. Bethge, H. Baumann, H. Jex, and F. Rauch (Vieweg, Braunschweig, 1980), p. 427.
[8]S. Mantl, W. Petry, K. Schroeder, and G. Vogl, Phys. Rev. B **27**, 5313 (1983).
[9]J. G. Mullen, Phys. Rev. **121**, 1649 (1961).
[10]J.-L. Bocquet, Acta Metall. **20**, 1347 (1972).
[11]S. K. Chen, M. B. Dutt, and A. K. Barua, Phys. Status Solidi A **45**, 657 (1978), containing further references on tracer studies of iron diffusion in copper.
[12]A. Larose and B. N. Brockhouse, Can. J. Phys. **54**, 1990 (1976).
[13]H. Wegener, *Der Mössbauereffekt und Seine Anwendung in Physik und Chemie* (Bibliographisches Institut, Mannheim, 1965).
[14]G. K. Shenoy, F. E. Wagner, G. M. Kalvius, in *Mössbauer Isomer Shifts,* edited by G. K. Shenoy and F. E. Wagner, (North-Holland, Amsterdam, 1978), p. 101.
[15]H. Schober and P. H. Dederichs, *Phonon States of Elements: Electron States and Fermi Surfaces of Alloys,* Group 3, Vol. 13a in *Landolt-Börnstein,* edited by P. H. Dederichs, H. Schober, and D. J. Sellmyer (Springer-Verlag, Berlin, 1981), p. 1.
[16]J. Rosén and G. Grimval, Phys. Rev. B **27**, 7199 (1983).
[17]R. O. Simmons and R. W. Baluffi, Phys. Rev. **129**, 1533 (1963).
[18]A. D. LeClaire, J. Nucl. Mater. **69**, 870 (1978).
[19]K. Ruebenbauer, Hyperfine Interact. **14**, 139 (1983).